Nuclear Instruments and Methods in Physics Research A299 (1990) 606–609
North-Holland

Range profiles and thermal release of ^{3}He implanted into various nickel-based amorphous alloys

Kenan Ünlü * and Dietrich H. Vincent

Department of Nuclear Engineering, University of Michigan, Ann Arbor, MI 48109, USA

The behavior of ^{3}He in the amorphous alloys $Ni_{75.1}Cr_{14}P_{10.1}C_{0.08}$, $Ni_{63.5}Zr_{36.5}$ and $Ni_{87.7}P_{12.3}$ is investigated. The samples were implanted with 150 keV ^{3}He ions with doses of 1×10^{16} and 5×10^{16} ^{3}He/cm^2. The samples were isochronally annealed at several consecutive stages up to their crystallization temperatures. After each annealing stage, ^{3}He depth profiles were measured by a thermal-neutron-induced nuclear-reaction technique called neutron depth profiling (NDP). The maximum ^{3}He release (~ 20%) was observed for the $Ni_{63.5}Zr_{36.5}$ sample and it occurred before crystallization. Smaller but measurable amounts of ^{3}He were released from most other combinations of sample material and implant doses The ^{3}He release that we observed is controlled by a detrapping process, and there are indications that it is dependent on the implantation dose. In addition to ^{3}He release measurements, our study yielded a determination of projected depths of ^{3}He ions with an initial energy of 150 keV in the alloys studied. The most probable range values are: 320 ± 21 nm for $Ni_{75.1}Cr_{14}P_{10.1}C_{0.08}$, 378 ± 34 nm for $Ni_{63.5}Zr_{36.5}$ and 375 ± 29 nm for $Ni_{87.7}P_{12.3}$.

1. Introduction

Materials problems anticipated for first-wall materials in fusion reactors, especially radiation-induced blistering and physical sputtering due to helium irradiation, have spurred an increasing interest in the behavior of helium in amorphous alloys. Since amorphous alloys have considerable resistance to surface erosion under helium bombardment [1–3], and exhibit desirable mechanical and chemical properties as compared with their crystalline counterparts [4–7], they have become potential candidates for various applications in future fusion reactors. Because of this, there is an active interest in the behavior of helium in amorphous alloys. However, most of the studies on helium in amorphous alloys concentrate on bubble formation, blistering and/or flaking for various energies and doses of helium irradiation. The purpose of these studies is usually to find out the critical implantation doses for blister formation. Consequently surface features are examined by scanning electron microscope (SEM) and subsurface microstructural changes are investigated by electron diffraction using a transmission electron microscope (TEM). The helium concentration as a function of depth is not usually measured. To the best of our knowledge the only depth profiling measurement was performed by Jäger et al. [8] using the ^{3}He(d, α)^{1}H reaction method. However, this method was used in conjunction with a multiple-energy implantation.

This paper will present the first ^{3}He depth-profiling measurements in various amorphous alloys, namely $Ni_{75.1}Cr_{14}P_{10.1}C_{0.08}$, $Ni_{63.5}Zr_{36.5}$ and $Ni_{87.7}P_{12.3}$ using a thermal-neutron-induced nuclear-reaction technique called neutron depth profiling (NDP). The NDP technique was originally developed in 1972 by Ziegler et al. [9]. The method determines a ^{3}He concentration profile from the measured energy distribution of emitted protons produced by the reaction ^{3}He(n, p)^{3}H when a beam of thermal neutrons passes through a sample. By comparing the ^{3}He depth profiles before and after a number of annealing stages, ^{3}He migration or loss can be determined as a function of annealing temperature.

2. Experimental

Three different amorphous alloys were used in this study. Samples of $Ni_{75.1}Cr_{14}P_{10.1}C_{0.08}$ and $Ni_{63.5}Zr_{36.5}$ were obtained from Allied Chemical Metglas Products and Allied Corporate Technology, respectively. They were produced by a liquid-quenching technique. The $Ni_{87.7}P_{12.3}$ sample was prepared, using electrodeposition, by Dr. Ferenc Paszti and Dr. Enico Toth-Kadar of the Hungarian Academy of Science. All samples were mechanically polished and the sample surface was examined using an optical microscope and a SEM. After polishing, all of the samples were checked by X-ray diffractometer and by electron diffraction to look for structural changes, and to ensure that they still had an

* Present address: University of Texas at Austin, Nuclear Engineering Teaching Laboratory, Balcones Research Center, Austin, TX 78712, USA.

0168-9002/90/$03.50

amorphous structure. The polished samples were implanted with 150 keV ^{3}He ions in a Varian Extrion high-current accelerator (Model 200-20A2). Doses were 1×10^{16} and 5×10^{16} ^{3}He/cm^2, i.e. low compared with those used in previous studies. After implantation, the samples were isochronally annealed at several consecutive stages up to their crystallization temperatures. The thermal treatments were performed in a Lindberg heavy-duty tube furnace. The annealing time was 20 min for each stage. To prevent oxidation and surface buildup during annealing, all samples were sealed in a quartz tube, and an inert nitrogen atmosphere was used. After each annealing stage, the ^{3}He depth distribution and relative concentration were measured by the NDP facility at the Ford Nuclear Reactor (FNR) of the University of Michigan. The FNR is an open-pool research reactor operating at a 2 MW power level. The final collimated beam comes from a 1.2 cm $\times$ 1.3 cm aperture made out of 4 in. of lead and 3/16 in. of cadmium. The measured neutron beam intensity at the aperture was 1.5×10^7 neutrons/(cm^2 s). A description of the NDP facility at FNR can be found in ref. [10]. For data acquisition, standard pulse-height analysis electronics were used. Fig. 1a shows a diagram of the data acquisition and analysis electronics. A gold-plated surface-barrier silicon detector was used to measure the energy distribution of protons escaping from the sample. The detector was an ORTEC AE-13-50-100 with a 50 mm^2 active area and had a 40 μg/cm^2 layer of gold on the front face. A precision reference pulse was fed into the detector's preamplifier to monitor system noise and possible gain shifts. The pulse height distribution was measured by an ORTEC 7150 multichannel analyzer. The neutron beam intensity was monitored with a parallel-plate fission chamber. The fission chamber provided the normalization of the neutron beam intensity and integration of the neutron exposure during analysis. Electronics used for the chamber are illustrated in fig. 1b. The discriminator output pulses were recorded in a ORTEC 871 Timer and Counter which gave a visual indication of the beam intensity during analysis and recorded the real time and integrated neutron exposure. Counting statistics were considered satisfactory at about 2.0×10^8 and 3.5×10^8 fission-chamber monitor counts for high- and low-dose samples, respectively. The exposure time necessary to achieve these total fluences were 38 and 66 h.

3. Results and discussions

A proton energy spectrum was obtained by measuring the residual energy of protons emerging from the surface of the sample with a surface-barrier detector. The energy of each proton emerging from the sample is related to the depth of the helium atom from which it originated by the characteristic proton stopping power in the sample material. Values of the stopping power for

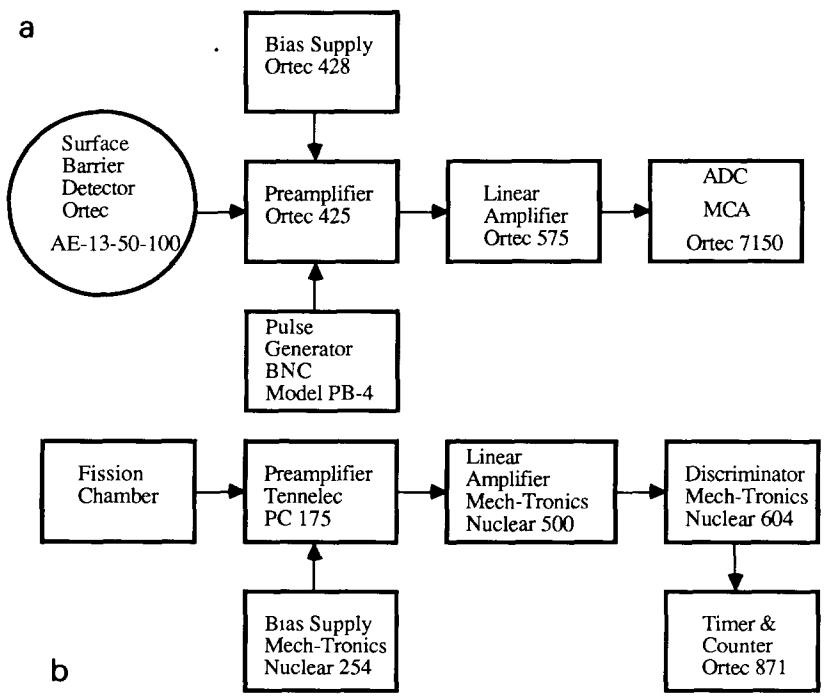

Fig. 1. Schematic of the NDP data-acquisition and -analysis electronics: (a) target chamber, (b) fission chamber.

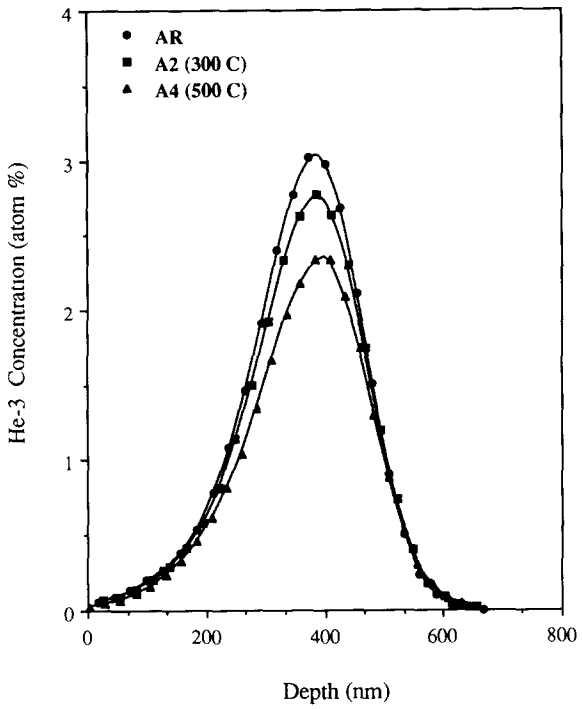

Fig. 2. Depth profiles of an isochronally annealed $Ni_{63.5}Zr_{36.5}$ sample. The annealing time was 20 minutes.

protons in the amorphous samples were obtained from Bragg's-law calculations in conjunction with Andersen's and Ziegler's tabulated data on elemental stopping powers [11]. The relative ^{3}He concentration in the annealed samples was determined by comparing the proton count rate obtained from each sample with that from the as-received sample. For the as-received samples the total dose was assumed to be equal to the nominal implantation dose.

After converting the channel numbers to the corresponding depth and the number of counts to relative ^{3}He concentration, the depth-concentration peaks were plotted and the lowest four moments of the depth distribution were calculated via a computer program. The sample status, the heat treatment histories, the first moment of the peak (the projected depth [nm]), the standard deviation, skewness and kurtosis (derived from the second, third and fourth moment, respectively) for the $Ni_{63.5}Zr_{36.5}$ sample (high-dose implant) are tabulated in table 1. The depth–concentration peak for the same sample is presented in fig. 2. The label AR (as-received) indicates the sample after implantation and before any heat treatment. The labels A1, A2, A3 and A4 refer to the first, second, third and fourth annealing states, respectively. The retained helium dose for every AR sample is assumed to be equal to the nominal implantation dose. After every annealing step, the amount of helium retained in a sample was determined by comparison with the initial implantation dose. The maximum ^{3}He release ($\sim 20\%$) was observed for the $Ni_{63.5}Zr_{36.5}$ sample with the high implantation dose, and it occurred before crystallization. Smaller but measurable amounts of ^{3}He were released from other combinations of sample material and implant doses we investigated. Although there was no substantial amount of ^{3}He release observed for all samples, one can discern a concentration dependence of the release. The high-dose samples released more helium than the low-dose samples. A similar behavior is also reported by several researchers for various crystalline metals [12,13].

The depth profiles shown in fig. 2 for various annealing stages are quite typical for helium release by a detrapping mechanism: once the temperature of the sample is high enough to release some of the helium atoms from the sites at which they are trapped, the atoms will rapidly escape from the sample. In this case the depth profile after annealing will show a uniformly reduced concentration over the whole profile without any broadening of the distribution. If the helium motion in the material were determined by pure diffusion, one would expect an increasing broadening of the profile as the annealing temperature increases. As may be seen in fig. 2 such broadening did not occur. Others have reported that the helium behavior in crystalline metals or alloys is likewise controlled by a pure detrapping mechanism [14–16].

An alternative method to study helium motion at elevated temperatures is isothermal annealing, where the annealing temperature is kept constant and the annealing times at that temperature are varied. We studied one of our samples ($Ni_{63.5}Zr_{36.5}$, high-dose im-

Table 1
Annealing data for a $Ni_{63.5}Zr_{36.5}$ sample with high-dose implant

Status	Annealing temp [°C]	Retained dose [$\times 10^{16}$ ^{3}He/cm^2]	Retained dose [%]	Projected depth [nm]	Standard deviation [nm]	Skewness	Kurtosis
AR	20	5.00 ± 0.11	100.0	360	100.53	−0.540	3.50
A1	200	4.76 ± 0.13	95.2	395	99.00	−0.545	3.45
A2	300	4.68 ± 0.11	93.6	364	101.20	−0.468	3.26
A3	400	4.48 ± 0.11	89.6	397	103.84	−0.583	3 50
A4	500	4.03 ± 0.11	80.7	368	103.51	−0 440	3.27

plant) by isothermally annealing it at 300 °C for 4 and 14 h. In this case, the change in the depth profiles is also in agreement with a pure detrapping mechanism, even though the profile for the maximum annealing time extends somewhat beyond the AR profile at deeper depth. We interpret this behavior as retrapping of helium released from its original trapping sites.

As an additional result this study yielded experimental values for the projected range of 150 keV ^{3}He in our amorphous samples. The most probable range values are: 320 ± 21 nm for $Ni_{75.1}Cr_{14}P_{10.1}C_{0.08}$, 378 ± 34 nm for $Ni_{63.5}Zr_{36.5}$ and 375 ± 29 nm for $Ni_{87.7}P_{12.3}$. Heretofore only calculated values for the projected range of ^{3}He in amorphous alloys were listed. One of these calculations [17] matches our experiments in material ($Ni_{63.5}Zr_{36.5}$) and implantation energy. However, that calculated range is ~25% larger than our measured value. While there is a wealth of data on ranges and stopping powers of ^{4}He in elemental matter [18], actual data on ^{3}He ranges are still rather sparse.

Neutron depth profiling has been found to be a valuable nondestructive technique to quantitatively observe the ^{3}He distributions in various amorphous alloys upon consecutive annealing stages. The amorphous alloys used in this study showed a measurable ^{3}He release (up to ~20%) before crystallization. The detrapping process appears to be the mechanism behind the ^{3}He release. There is also an indication of a dependence of the amount released on implantation dose. The projected depth of ^{3}He ions with an initial energy of 150 keV in the alloys studied was determined. Along with the neutron beam analysis the surface features and microstructural changes of our samples were studied systematically by scanning electron microscopy and electron diffraction. The results of these studies will be published elsewhere.

Acknowledgements

The authors would like to thank Dr. H.H. Lieberman of Allied Corporate Technology and Drs. Ferenc Paszti and Enico Toth-Kadar of Hungarian Academy of Sciences for supplying the amorphous alloy samples used in this study. Appreciation is extended to Dr. Kenneth Grabowski of the Naval Research Laboratory for performing the ^{3}He implants. Finally, we thank the Phoenix Memorial Laboratory/Ford Nuclear Reactor staff for accommodating the experimental needs for the neutron depth profiling facility.

References

[1] A. Manuaba, F. Paszti, L. Pogany, M. Fried, E. Kotai, G. Mexey, T. Lohner, I. Lovas, L. Pocs and J. Gyulai, Nucl. Instr. and Meth. 199 (1982) 409
[2] F. Paszti, M. Fried, L. Pogany, A. Manuaba, G. Mezey, E. Kotai, I. Lovas, T. Lohner and L. Pocs, Nucl. Instr. and Meth. 209/210 (1983) 273.
[3] A.K. Tyagi, R.V. Nandedkar and K. Krishan, J. Nucl. Mater. 114 (1983) 181.
[4] T. Masumoto and R. Maddin, Mater. Sci. Eng. 19 (1975) 1
[5] J.C.M. Li, in: Treatise of Material Science and Technology, ed. H. Herman, vol. 20 (Academic Press, New York, 1981) p. 326.
[6] T.K.G. Namboodhiri, in: Metallic Glasses: Production, Properties and Application, ed. T.R. Anantharaman (Trans. Tech. Publications Ltd., Switzerland, 1984) p. 203.
[7] R. Hasegawa, Glassy Metals: Magnetic, Chemical and Structural Properties (CRC Press, Boca Raton, 1983).
[8] W. Jäger and J. Roth, Nucl. Instr. and Meth. 182/183 (1981) 975.
[9] J.F. Ziegler, G.W. Cole and J.E.E. Baglin, J. Appl. Phys. 43 (1972) 3809.
[10] K. Ünlü, Ph.D. Dissertation (Dept. of Nuclear Engineering, Univ. of Michigan, 1989).
[11] H.H. Andersen and J.F. Ziegler, The Stopping and Ranges of Ions in Matter, vol. 3 (Pergamon Press, New York, 1977)
[12] J.P. Biersack, D. Fink, R.A. Henkelman and K. Müller, J. Nucl. Mater. 85/86 (1979) 1165.
[13] J.T. Maki, Ph.D. Dissertation (Dept. of Nuclear Engineering, Univ. of Michigan, 1987)
[14] J.P. Biersack and D. Fink, Proc. 8th Symp. on Fusion Technology, Luxembourg, Euratom (EUR 5182 e) (1974) p. 907.
[15] J. Roth, S.T. Picraux, W. Eckstein, J. Bottinger and R. Behrisch, J Nucl. Mater. 63 (1976) 120.
[16] J. Ehrenberg, B.M.U. Sherzer and R. Behrisch, Radiat. Eff. 78 (1983) 405.
[17] A.K. Tyagi and R.V. Nandedkar, J. Nucl. Mater 132 (1985) 62.
[18] J.F. Ziegler, Helium Stopping Powers and Ranges in All Elemental Matter, vol. 4 of: Stopping and Ranges of Ions in Matter (Pergamon Press, New York, 1977).